Published in final edited form as:

Mol Microbiol. 2021 June ; 115(6): 1170–1180. doi:10.1111/mmi.14660.

MltG activity antagonizes cell wall synthesis by both types of peptidoglycan polymerases in *Escherichia coli*

Jessica L. Bohrhunter[1], **Patricia D.A. Rohs**[1], **Grasiela Torres**[1], **Rachel Yunck**[1], **Thomas G. Bernhardt**[1,2,*]

[1]Department of Microbiology, Harvard Medical School, Boston, Massachusetts 02115, USA

[2]Howard Hughes Medical Institute

SUMMARY

Bacterial cells are surrounded by a peptidoglycan (PG) cell wall. This structure is essential for cell integrity and its biogenesis pathway is a key antibiotic target. Most bacteria utilize two types of synthases that polymerize glycan strands and crosslink them: class A penicillin-binding proteins (aPBPs) and complexes of SEDS proteins and class B PBPs (bPBPs). Although the enzymatic steps of PG synthesis are well characterized, the steps involved in terminating PG glycan polymerization remain poorly understood. A few years ago, the conserved lytic transglycosylase MltG was identified as a potential terminase for PG synthesis in *Escherichia coli.* However, characterization of the *in vivo* function of MltG was hampered by the lack of a growth or morphological phenotype in Δ*mltG* cells. Here, we report the isolation of MltG-defective mutants as suppressors of lethal deficits in either aPBP or SEDS/bPBP PG synthase activity. We used this phenotype to perform a domain-function analysis for MltG, which revealed that access to the inner membrane is important for its *in vivo* activity. Overall, our results support a model in which MltG functions as a terminase for both classes of PG synthases by cleaving PG glycans as they are being actively synthesized.

Keywords

peptidoglycan; penicillin; cell wall; lytic transglycosylase; cell envelope

INTRODUCTION

Most bacteria fortify their cytoplasmic membrane with a cell wall layer that is essential for growth and survival (Höltje, 1998). The wall is build from a heteropolymer called peptidoglycan (PG), which consists of glycan strands with a repeating disaccharide unit of N-actelyglucosamine (GlcNAc) and N-acetylmuramic acid (MurNAc). Short peptide stems are attached to the MurNAc sugars and are used to make the inter-strand crosslinks that create the net-like structure of the PG layer.

*To whom correspondence should be addressed: Thomas G. Bernhardt, Howard Hughes Medical Institute, Harvard Medical School, Department of Microbiology, Boston, Massachusetts 02115, USA, thomas_bernhardt@hms.harvard.edu.

Two main types of synthases are responsible for assembling the PG matrix. The bifunctional class A penicillin binding proteins (aPBPs) have been known to be major synthetic enzymes for some time (Sauvage et al., 2008). They possess both PG glycosyltransferase (GT) activity to polymerize the glycan strands and transpeptidase (TP) activity to form the inter-strand crosslinks. In the last few years, it was discovered that proteins in the SEDS (Shape, Elongation, Division and Sporulation) family also have GT activity and function as PG polymerases (Meeske et al., 2016; Taguchi et al., 2019). Recent work has shown that these polymerases work in complex with crosslinking enzymes called class B penicillin binding proteins (bPBPs) to form a second class of bifunctional PG synthase (Cho et al., 2016; Rohs et al., 2018; Taguchi et al., 2019). In *Escherichia coli*, PBP1a and PBP1b are the critical aPBPs for PG biogenesis (Kato et al., 1985; Yousif et al., 1985), and RodA/PBP2 and FtsW/PBP3 form the SEDS-bPBP synthases of the elongation and division machineries, respectively (Meeske et al., 2016; Cho et al., 2016; Rohs et al., 2018; Taguchi et al., 2019).

Although PG glycan synthesis has been reconstituted *in vitro* for both types of PG synthases (Ishino et al., 1980; Nakagawa et al., 1984; Höltje, 1998; Ye et al., 2001; Bertsche et al., 2005; Meeske et al., 2016; Rohs et al., 2018; Taguchi et al., 2019), it remains unclear how the polymerization reaction is terminated. The substrate for the synthetic enzymes is the PG precursor lipid II, which consists of a MurNAc(peptide)-GlcNAc monomer unit linked by a pyrophosphate to a polyprenol lipid called undecaprenol (Höltje, 1998). The final product of polymerization by the synthases is therefore a glycan chain anchored to the membrane at one end by the undecaprenol carrier (Fig. 1). Thus, additional steps are likely required to liberate the nascent glycan from the membrane and allow completion of its insertion into the growing PG matrix. The PG glycans in *E. coli* and other bacteria are capped by MurNAc sugars with a 1,6-anhydro ring (^{Anh}MurNAc) (Höltje, 1998) (Fig. 1). Enzymes called lytic transglycosylases (LTs) form these moieties in the process of cutting glycan strands (Scheurwater et al., 2008). Therefore, LTs have long been thought to facilitate the last step of glycan chain incorporation into the wall (Kraft et al., 1998; Heidrich et al., 2002) (Fig. 1). These enzymes may either act by cleaving and releasing glycan strands from the membrane after their polymerization is completed by the synthase, or they may function as terminases, engaging with actively polymerizing synthases to cut the growing strand and terminate its synthesis.

Several years ago, we identified MltG as a new LT enzyme that is broadly conserved in bacteria (Yunck et al., 2015). Among the LTs in *E. coli*, MltG was unique in that it was found to be localized to the inner membrane whereas all previously characterized LTs were found to be outer membrane lipoproteins (MltA-F) or soluble periplasmic proteins (Slt) (van Heijenoort, 2011; Jorgenson et al., 2014; Yunck et al., 2015). Biochemical analysis indicated that MltG had endoglycolytic activity that allowed it to cleave within glycan strands (Yunck et al., 2015). Cell walls isolated from a mutant lacking MltG were also found to have glycan strands that were, on average, longer than those from wild-type cell walls (Yunck et al., 2015). These results coupled with its inner membrane localization suggested that MltG might be an LT enzyme with terminase activity *in vivo*. However, the lack of a growth or morphological phenotype for Δ*mltG* mutants has hampered further exploration of MltG function in *E. coli* cells.

In this report, we present results of genetic selections for suppressors of cell wall synthesis defects resulting from a deficit in either aPBP or SEDS/bPBP synthase activity. In both cases, mutants inactivating *mltG* were isolated. We took advantage of one of these phenotypes to perform a domain-function analysis for MltG, which revealed that access to the inner membrane is important for its *in vivo* activity. Overall, our results indicate that MltG works in opposition to both classes of PG synthases in *E. coli*, an activity consistent with it functioning as a terminase that processes glycan strands as they are being actively synthesized.

RESULTS

MltG inactivation suppresses growth defects resulting from an aPBP deficiency

The aPBP synthases PBP1a and PBP1b form a synthetic lethal pair in *E. coli* (Kato et al., 1985; Yousif et al., 1985). The synthases are individually dispensable, but their simultaneous inactivation results in rapid cell lysis. Each synthase requires an outer membrane lipoprotein co-factor for their *in vivo* activity (Paradis-Bleau et al., 2010; Typas et al., 2010). LpoA promotes PBP1a activity, and PBP1b is activated by the unrelated lipoprotein LpoB (Paradis-Bleau et al., 2010; Typas et al., 2010). In a previous report investigating the mechanism of PBP1b activation by LpoB, we identified variants of PBP1b that bypass its LpoB requirement for function (Markovski et al., 2016). One of the variants, PBP1b(E313D), was found to be capable of supporting growth of a strain deleted for both *ponA* (encoding PBP1a) and *lpoB* (Markovski et al., 2016), a combination of mutations that is normally lethal due to both aPBPs being inactivated (Paradis-Bleau et al., 2010; Typas et al., 2010). However, growth of this suppressed strain (MM119) was salt-sensitive (Markovski et al., 2016). It formed colonies on LB medium without NaCl (LB0N), but failed to grow on LB containing 1-1.5% NaCl. Overproduction of PBP1b(E313D) from a plasmid was shown to suppress the salt-sensitive growth of MM119 [*ponB(E313D)* Δ*ponA* Δ*lpoB*], suggesting that the growth defect resulted from a deficit in cellular aPBP activity (Markovski et al., 2016). Based on this finding, we reasoned that the isolation of suppressors that promote the growth of MM119 on LB with 1.5% NaCl might identify additional factors that promote or antagonize PBP1b activity.

For the suppressor selection, strain MM119 was subjected to transposon mutagenesis using the transposome Ez-Tn5 (Epicentre). The resulting mutant library was then plated on LB 1.5% NaCl. Several suppressors were isolated, and the location of the inserted transposon in each mutant was mapped using arbitrarily-primed PCR. Among the suppressors, 16 had insertions in *hrpB*, 5 had insertions in *mltG* (Fig. 2A), one had an insertion in *pgm*, and one had an insertion in *ycbB.* The *hprB* gene is located immediately upstream of *ponB.* Because we previously showed that overproduction of PBP1b(E313D) from a plasmid suppressed the salt sensitivity of MM119 (Markovski et al., 2016), we suspected that transposon insertions in *hprB* were similarly promoting the growth of MM119 by increasing PBP1b production. We therefore did not study these suppressors further. Of the remaining genes identified in the suppressor selection, only a deletion-insertion allele of *mltG* (Δ*mltG::Cam*^{R}) promoted the growth of MM119 on LB 1.5% NaCl agar (Fig. 2B). Deletion-insertion alleles of *pgm* and *ycbB* (Δ*pcm::Kan*^{R} and Δ*ycbB::Kan*^{R}*)* from the Keio collection were ineffective.

We therefore focused this study on further characterizing the suppressing activity of MltG inactivation.

To determine whether the suppression phenotype of the Δ*mltG::Cam*^{R} allele was due to the loss of MltG catalytic activity or required the complete absence of the MltG polypeptide, we introduced the *mltG(E218Q)* into MM119. This allele encodes a catalytically inactive MltG protein (Yunck et al., 2015). It was also found to suppress the salt sensitivity of MM119, indicating that loss of MltG catalytic activity was sufficient to rescue the aPBP activity deficit of this strain (Fig. 2C). We were curious whether the inactivation of other LTs would have a similar suppressive effect on MM119 growth. Single deletions of other LT-encoding genes were therefore introduced into this background, but only the Δ*mltG::Cam*^{R} allele was found to be capable of promoting the growth of MM119 on LB 1.5% NaCl agar (Fig. 3).

We next investigated whether MltG inactivation was capable of suppressing the growth defect of other strains deficient in aPBP activity. We first tested a strain background (CB68) in which both *lpoA* and *lpoB* were deleted and a second copy of *lpoB* was expresses under control of the lactose promoter from an ectopic site [Δ*lpoA* Δ*lpoB* (P_{lac}::*lpoB*)]. In the absence of IPTG, this strain will be depleted of LpoB. The strain plates at a reduced efficiency under this depletion condition because it also lacks LpoA and thus presumably cannot effectively activate either aPBP (Fig. 4A) (Paradis-Bleau et al., 2010). Inactivating MltG was also found to rescue the plating defect of this aPBP deficient strain on medium lacking IPTG (Fig. 4A). However, disrupting MltG function was unable to rescue the plating defect resulting from LpoB depletion in cells lacking PBP1a instead of LpoA (Fig. 4A). We infer from this result that a certain threshold of aPBP activity is required for growth even when MltG is inactivated. In this case, poorly activated PBP1b in LpoB-depleted cells appears to be insufficient for growth unless cells also retain unactivated PBP1a, which presumably retains enough basal activity without LpoA to support viability.

To investigate whether the inactivation of other LTs is capable of suppressing the growth defect of LpoB depletion in cells lacking LpoA, deletion alleles of several LT-encoding genes were introduced into the CB56 background [Δ*lpoA* Δ*lpoB* (P_{lac}::*lpoB*)]. The viability defect of CB56 in the absence of IPTG is less severe than the salt-dependent growth phenotype of MM119 [*ponB(E313D)* Δ*ponA* Δ*lpoB*], and it was found to be suppressed by deletion of *mltA* or *mltB* in addition to *mltG* (Fig. 4B). Thus, among the LTs in *E. coli*, MltG appears to play the most significant role in opposing PG synthesis by the aPBPs with MltA and MltB also counterbalancing synthesis to some degree, which is consistent with previous work implicating them as playing major roles in PG turnover during growth (Kraft et al., 1999).

An MltG truncation suppresses defects in the Rod system

MltG was also identified as an antagonist of SEDS-bPBP complexes in a parallel investigation of the regulation of RodA-PBP2. This synthase is essential for the function of the Rod system (elongasome) responsible for cell elongation and shape maintenance (Typas et al., 2012; Meeske et al., 2016; Cho et al., 2016). The Rod system is organized by filaments of the actin-like MreB protein and includes the membrane proteins MreC, MreD, and RodZ in addition to the RodA-PBP2 synthase (Typas et al., 2012). We recently

identified a non-functional variant of MreC, MreC(R292H) (Rohs et al., 2018). Cells encoding the *mreC(R292H)* allele at the native *mre* locus have a severe Rod system defect. They are amorphous and must be maintained on minimal medium, a condition permissive for the growth of cells defective for the Rod system (Bendezú and de Boer, 2008; Rohs et al., 2018) (Fig. 5A–B). To better understand the nature of the Rod system defect in these cells, we isolated spontaneous suppressors that restored viability on LB medium where Rod system inactivation is normally lethal (Bendezú and de Boer, 2008). One class of mutants isolated produced an altered PBP2 protein that was found to activate PG synthesis by the RodA/PBP2 synthase (Rohs et al., 2018). This finding suggested that the defect in *mreC(R292H)* cells is reduced PG synthesis activity by the Rod system. Another suppressor isolated that was not previously reported was a frameshift mutation in *mltG* at codon 133, *mltG(I133fs).* This lesion promotes the growth of *mreC(R292H)* cells on LB (Fig. 5A), and partially corrects their shape defect (Fig. 5B). Although expression of *mltG* from a plasmid has no affect on the growth of wild-type cells, it complements the *mltG(I133fs)* defect by restoring the plating and shape defects of *mreC(R292H) mltG(I133fs*) cells (Fig. 5C–D).

Surprisingly, a deletion allele of *mltG* did not suppress the growth defect of *mreC(R292H)* mutants on LB (Fig. S1A). One possible explanation for the differential suppression activity displayed by the *mltG* alleles is that the fragment of MltG produced in cells with the *mltG(I133fs*) mutation provides a function required for suppression of *mreC(R292H).* However, expression of a catalytically defective *mltG(E218Q)* allele or an *mltG(1-133*) truncation did not promote growth of a *mreC(R292H)* Δ*mltG* strain on LB (Fig. S1B). We therefore suspect that the *mltG* deletion may affect the expression of downstream essential genes *tmk* and *holB.* We have not observed any negative growth defects in cells with an *mltG* deletion allele alone (Yunck et al., 2015), but the potential effects of the *mltG* deletion on *tmk* and *holB* expression may exacerbate the severe growth defects caused by the *mreC(R292H)* allele to prevent the expected suppression phenotype. Although further work will be required to test this hypothesis, the results with the *mreC(R292H) mltG(I133fs*) cells strongly suggest that the loss of MltG function can suppress defects in the Rod system as well as defects in aPBP activity.

Evidence that MltG only associates with active PG polymerases

Using bacterial two-hybrid (BACTH) analysis (Karimova et al., 1998), we previously detected an interaction between MltG and PBP1b (Fig. 6A) (Yunck et al., 2015). Given the genetic connection of MltG with Rod complex activity, we also wondered whether MltG might also associate with this machinery. Indeed, a positive interaction signal was detected with RodA (Fig. 6B). Given that PBP1b and RodA are members of entirely different classes of PG polymerases and do not share any sequence relatedness, it was surprising to see that MltG showed a positive BACTH signal with both proteins. We therefore considered the possibility that rather than representing a protein-protein interaction, the BACTH results might be reporting on an interaction between MltG and nascent glycans in the process of being polymerized by the synthases. To test this hypothesis, we generated BACTH fusions to PBP1b and RodA variants defective for polymerase activity. Indeed, the BACTH interaction signal with MltG was dramatically reduced for these fusions (Fig. 6A–B). In the case of PBP1b, the GT inactivated variant PBP1b(E233Q) remained capable of producing a positive

interaction signal with wild-type PBP1b. Prior studies also indicate that the GT-defective RodA variant is dominant negative (Cho et al., 2016), indicating that the amino acid substitution that disrupts its polymerase activity does not affect its stability. We therefore infer that MltG is only capable of interacting with active PBP1b or RodA polymerases. Thus, MltG may either be recognizing an active conformation of the polymerases or associating with the glycan polymers they produce instead of participating in a direct protein-protein interaction with the synthases.

MltG domain function analysis

The discovery that MltG inactivation suppresses the salt sensitivity of MM119 provided us with a phenotypic assay to assess the domain requirements for the *in vivo* function of MltG. *E. coli* MltG has three domains: an N-terminal transmembrane domain (TMD), a predicted LysM PG binding domain, and the C-terminal YceG catalytic domain (PDB: 4IIW and 2r1f) (Yunck et al., 2015) (Fig. 7A). We wished to determine which of these domains contribute to MltG function. Additionally, because MltG is unique among *E. coli* LTs in being inner membrane localized (Yunck et al., 2015), we wanted to determine if this localization is required for its function.

For the analysis, an MM119 derivative lacking a chromosomal copy of *mltG* was constructed. Because its native MltG is inactivated, strain JLB93 [*ponB(E313D)* Δ*ponA* Δ*lpoB* Δ*mltG*], is viable on LB 1.5% NaCl unlike its parent MM119 (Fig. 7B). However, expression of *mltG*(WT) from a plasmid under P_{lac} control complemented the *mltG* deletion of JLB93 by restoring the growth defect when low concentrations of inducer were included in the medium (25 μM IPTG) (Fig. 7B). Even though immunoblotting indicated that MltG was overproduced from the plasmid relative to the barely detectable signal observed when it was expressed from the native locus (Fig. 7C), the growth defect induced by plasmid expression was specific for JLB93 [*ponB(E313D)* Δ*ponA* Δ*lpoB* Δ*mltG*]. Induction of *mltG*(WT) expression from the plasmid was not found to cause a growth defect in wild-type cells at any level of inducer (Fig. S2).

Production of MltG derivatives where an alternative TMD or a signal sequence for secretion to the periplasm replaced the native sequence also restored salt-sensitivity to JLB93, indicating that these variants are functional (Fig. 7B and C). In addition to replacing the native TMD with a normal secretion signal sequence, we also generated constructs where the TMD was substituted with the signal sequence for the lipoprotein Pal (Lloubès et al., 2001). Addition of the wild-type Pal sequence is expected to direct the lipidation of the protein following secretion and the subsequent targeting of the lipoprotein to the outer membrane (Tokuda and Matsuyama, 2004), and we have previously shown that this exact signal sequence promotes outer membrane targeting of fluorescent proteins (Yunck et al, 2015). Despite the accumulation of full-length protein, this ^{SS}Pal-MltG derivative was unable to complement the *mltG* deletion of JLB93 (Fig. 7B and C), presumably as a result of relocalization to the outer membrane. Alteration of the Pal signal sequence to change the two residues immediately following the lipidated Cys to Asp-Glu is predicted to form an inner membrane retention signal (Tokuda and Matsuyama, 2004; Yunck et al., 2015). We have previously confirmed this prediction by showing that the altered Pal sequence (^{SS}Pal**)

results in the retention of a fluorescent protein in the inner membrane (Yunck et al, 2015). Notably, this change in the signal sequence rendered the ^{SS}Pal**-MltG fusion construct functional in restoring the growth defect to JLB93 [*ponB(E313D)* Δ*ponA* Δ*lpoB* Δ*mltG*]. Importantly, none of the functional MltG derivatives affected the growth of wild-type cells, indicating that like MltG(WT), the growth defect they caused was specific for the JLB93 background. From these results, we conclude that, although the N-terminal TMD of MltG is not required for function, access to the inner membrane is, either as a soluble periplasmic protein or one with an alternative inner membrane anchor.

To test the requirement for the LysM domain for MltG function, we generated versions of the functional ^{SS}DsbA- and ^{SS}Pal**-MltG fusions in which this domain was deleted. Neither of these constructs was capable of complementing the Δ*mltG* phenotype of JLB93 [*ponB(E313D)* Δ*ponA* Δ*lpoB* Δ*mltG*]. Immunoblot analysis indicated that these constructs promoted the accumulation of significantly more protein than natively expressed *mltG.* Therefore, although it is difficult to rule out effects on protein folding due to the removal of the LysM domain, the results suggest that it is likely playing an important role in MltG function.

DISCUSSION

MltG was first identified in *E. coli* based on its lethal overexpression phenotype in cells lacking the aPBP PG synthase PBP1b (Yunck et al., 2015). It was subsequently characterized to be an inner-membrane protein with endolytic LT activity *in vitro.* These properties suggested that MltG might be one of the missing terminase enzymes that cleave nascent glycan strands to complete their synthesis and incorporation into the PG matrix (Yunck et al, 2015). Accordingly, MltG inactivation was found to increase the average glycan strand length in purified PG sacculi (Yunck et al, 2015). However, loss of MltG function was not found to result in a discernible growth or morphological phenotype, making it difficult to gain further insight into its *in vivo* role in PG synthesis. Here, we report the identification of *mltG* mutants as suppressors of PG synthesis defects. Mutants inactivated for MltG were found to restore growth to a strain with a lethal deficit in aPBP activity and a strain defective in the activity of the elongation system, which utilizes a SEDS/bPBP synthase. We used the former phenotype to perform a domain function analysis for MltG and found that its LysM domain is important for activity and that it requires access to the inner membrane for function. Based on the suppression phenotypes, we conclude that MltG activity works in opposition to the activity of both PG synthase classes in *E. coli*.

Published results from *Streptococcus pneumoniae* also suggest an antagonistic relationship between MltG activity and PG synthases (Tsui et al., 2016). Deletion mutants that inactivate components of the peripheral PG synthesis machinery in this bacterium, the equivalent of the Rod system in *E. coli* and other rod-shaped cells, are normally lethal (Land and Winkler, 2011). However, mutants inactivating ^{Sp}*mltG* were found to allow the deletion of genes encoding PBP2b and other components of the peripheral PG synthesis machinery (Tsui et al., 2016). Although this result parallels our finding that a frameshift allele of ^{Ec}*mltG* suppresses the defective *mreC*(R292H) allele in *E. coli*, the mechanisms of suppression are likely to be slightly different. The *E. coli* result suggests that the RodA-PBP2 synthase

of the Rod system remains partially functional in the *mreC*(R292H), but that MltG processing overwhelms the weak glycan synthesis activity resulting in the growth and shape defects. Accordingly, inactivation of MltG restores growth on non-permissive conditions and promotes cell elongation to partially restore rod shape. In *S. pneumoniae*, on the other hand, MltG inactivation suppresses deletions of genes encoding peripheral PG synthesis factors (Tsui et al., 2016) and is therefore unlikely to promote growth by supporting the activity of a partially functional machine. Instead, loss of MltG activity is likely boosting overall synthesis by other cellular systems in order to compensate for the loss of peripheral PG synthesis activity by RodA-PBP2b, the SEDS-bPBP equivalent of RodA-PBP2 in *E. coli.*

Another connection of MltG to PG synthesis identified in *S. pneumoniae* relates to the observed essentiality of the ^{Sp}*mltG* gene (Tsui et al., 2016). This essentiality was suppressed by inactivation of the aPBP ^{Sp}PBP1a (Tsui et al., 2016). Aberrant ^{Sp}PBP1a activity has been shown to be toxic to *S. pneumoniae* cells (Land and Winkler, 2011; Fenton et al., 2016). Therefore, like *E. coli*, the genetic relationship between ^{Sp}MltG and aPBP activity can be interpreted as antagonistic. However, in this case, loss of ^{Sp}MltG function may lead to overactive and therefore toxic levels of ^{Sp}PBP1a synthesis such that ^{Sp}PBP1a inactivation rescues the ^{Sp}MltG defect.

Because they break bonds in the PG matrix, all PG cleaving enzymes can naturally be thought to antagonize PG synthase activity. However, the apparent specificity by which MltG inactivation suppresses defects in PG synthesis in two quite different bacteria indicates that there is something special about the way in which MltG opposes synthesis. MltG was previously implicated in nascent glycan turnover in beta-lactam treated *E. coli* (Yunck et al., 2015), indicating that it is capable of processing newly synthesized PG material. However, if it were simply processing freshly completed glycans to liberate them from their lipid anchor, MltG activity would not be predicted to antagonize synthesis unless it also promoted a significant turnover of mature PG. This latter possibility seems unlikely given that the structure of MltG indicates that the active site of the membrane-anchored protein probably cannot even reach the mature PG layer (Fig. S3). Instead, we propose that MltG serves as a relatively robust antagonist of PG synthase activity because it is capable of processing nascent glycans undergoing active polymerization by the synthases, an activity supported by the the BACTH results in which MltG only generates a positive interaction signal with functional polymerases. Although further work will be required to investigate this possibility, the results presented here provide additional support for a terminase like function for MltG and provide genetic tools to continue investigating the poorly understood process by which PG glycan polymerization is completed in bacteria.

EXPERIMENTAL PROCEDURES

Bacterial strains, plasmids and media used

The bacterial strains used in this study are listed in Table S1 and are all derivatives of MG1655. All deletion constructs were sourced from the Keio collection (Baba et al., 2006), except for Δ*mltG*, which was constructed by recombineering in an earlier study (Yunck et al., 2015). Cultures were grown in LB medium (1% tryptone, 0.5% yeast extract) containing 0.5% NaCl, unless otherwise noted or minimal M9 media supplemented with 0.2%

casamino acids and 0.2% glucose. Media was supplemented with the antibiotics ampicillin (Amp), kanamycin (Kan), and chloramphenicol (Cm), as needed, at the concentrations noted. See figure legends for specific growth conditions used for each experiment.

The *mltG(E218Q)* allele was constructed via allelic exchange. A pir-dependent suicide plasmid pRY76 [*sacB* Cm^R *mltG(E218Q)*] was introduced into the recipient strain NP47 [$streptomycin^R$] by conjugative transfer from the donor strain SM10(λpir). Briefly, 100 μL of stationary phase culture of the donor and recipient strains were incubated together in 200 μL of LB broth for six hours at 37°C. Cells were then serially diluted and plated on LB agar supplemented with chloramphenicol (10 μg/mL) and streptomycin (100 μg/mL), and incubated at 30°C for 1-4 days to select for integration of pRY47 into the chromosome via a single cross-over. Exconjugants were purified on the same medium. An overnight culture was then grown from a single purified exconjugant colony, normalized to an OD_{600} of 1, and plated on LB agar supplemented with 6% sucrose. The plate was incubated at 30 °C overnight to select for recombinants that lost the *sacB*-containing plasmid via a second cross-over. Recombinants were then patched on LB agar supplemented with 6% sucrose or chloramphenicol (10 μg/mL) to confirm loss of the integrated vector. Allelic replacement was verified by PCR followed by Sanger sequencing.

Plasmids used in this study are listed in Table S2 and construction information is detailed in Supplemental Material. PCR was performed using Q5 polymerase (NEB) for cloning purposes and GoTaq polymerase (Promega) for diagnostic purposes, both according to the manufacturer's protocol. Plasmid DNA was purified using the Zymo Research Zyppy plasmid miniprep kit. PCR fragments were purified using the Qiagen PCR purification kit.

Selection for suppressors of MM119 salt sensitivity

Strain MM119 [*ponB*(E313D) Δ*lpoB::frt* Δ*ponA::frt*] was mutagenized with the Ez-Tn5 <Kan-2> transposome (Epicentre) as previously described (Bernhardt and de Boer, 2004). Mutants were selected on LB0N agar supplemented with Kan (25 μg/mL) at 30°C, yielding a library with approximately 10^5 independent insertion mutants. The mutant library was harvested by scraping colonies from the agar surface and suspending them in LB0N broth. The suspended cells were then plated on LB 1.5% NaCl agar and incubated at 30°C to isolate suppressors. A subset of the surviving colonies were purified on LB 1.5% NaCl agar at 30°C.

Transposon insertion sites in the suppressors were mapped using arbitrarily primed PCR as described previously (Bernhardt and de Boer, 2004). PCR to amplify the transposon junction was performed using Taq polymerase (NEB) and templated by a single isolated colony suspended directly in the PCR reaction mixture. The arbitrarily priming primer ARB1 (5'-GGCCACGCGTCGACTAGTACNNNNNNNNNNGATGCd-3') and the transposon specific primer EzTn-up2 (5'-CGATAGATTGTCGCACCTGATTGC-3') were used. A second, nested PCR was then performed using the primers ARB2 (5'-GGCCACGCGTCGACTAGTAC-3') and EzTn-up (5'-TTGAATATGGCTCATAACACCCCTTG-3'). PCR fragments were then purified using the Qiagen PCR purification kit and submitted for Sanger sequencing at the Dana-Farber/ Harvard Cancer Center Sequencing Facility using the EzTn-up primer.

Selection for suppressors of the Rod system defect caused by MreC(R292H)

This suppressor selection has been previously reported elsewhere (Rohs et al., 2018). Briefly, cultures of PR5 [*mreC(R292H)*] were plated on LB at 30° C. Surviving colonies were screened for sensitivity to A22, to ensure they had restored Rod system function. A22 sensitive mutants were then visually screened to confirm restoration of rod shape. Finally, suppressor mutations were identified by whole genome sequencing using the Miseq System (Illumina). Strain PR36 was found to have one change, an 1 bp deletion at codon 133 of *mltG* creating a frameshift. The resulting mutant is predicted to express MltG(1-132) with an additional extension of 4 amino acids from the frameshift.

Bacterial two hybrid

BACTH plasmids were co-transformed into BTH101 (Karimova et al., 1998). Transformants were grown overnight at 30°C in LB with 50-100 μg/mL ampicillin, 25-50 μg/mL kanamycin and 1 mM IPTG. An aliquot (5 μl) of each stationary phase culture was spotted on LB agar containing 50-100 μg/mL ampicillin, 25-50 μg/mL kanamycin, 1 mM IPTG, and 80 μg/mL X-gal. Plates were incubated at room temperature for 24-48 hours. After incubation, plates were stored at 4°C for at least 18 hours to assist color development before being imaged.

Immunoblotting

Whole-cell extracts were prepared by resuspension of cells in SDS-PAGE buffer to an OD_{600} of 20 followed by incubation at 95°C for 5 minutes. The protein concentration of each extract was determined using the non-interfering protein assay (Genotech) according to the manufacturer's instructions, and then normalized to 1 mg/mL. A total of 15 μg of protein from each extract was separated on a 12% SDS-PAGE gel (with 4% stacking gel). Proteins were then transferred to a PVDF membrane (Bio Rad) and the membrane was blocked with 2% milk in TBST (0.05% Tween 20, 10 mM TrisHCl, pH 7.5, 100 mM NaCl). The membrane was incubated with primary polyclonal anti-MltG antibodies (Yunck et al., 2015), pre-cleared of nonspecific antibodies by incubation for 1 hour with Δ*mltG* cell lysates. The pre-cleared preparation was diluted 1:5000 in 1% milk in TBST and incubated with the blot overnight with gentle agitation at 4°C. The primary antibody solution was then removed and the membrane was quickly rinsed with TBST and washed three times with 50ml TBST for 10 minutes each wash. After the final wash, the membrane was incubated with gentle agitation for 1 hour at room temperature with secondary goat anti-rabbit antibodies conjugated to horseradish peroxidase (Rockland) diluted 1:40,000 in 1% milk in TBST. After incubation, the secondary antibody solution was discarded and the membrane was quickly rinsed twice with TBST and washed twice with 50ml TBST for 5 minutes each. The blot was developed using the Super Signal West Pico system (Pierce) according to the manufacturer's protocol. Chemiluminescence was detected using a Amersham Imager 600 (GE Life Sciences).

Supplementary Material

Refer to Web version on PubMed Central for supplementary material.

ACKNOWLEDGEMENTS

The authors would like to thank all members of the Bernhardt and Rudner labs as well as Suzanne Walker for advice and helpful discussions. We would also like to thank Cynthia Hale and Piet de Boer for providing some of the BACTH constructs. This work was supported by the National Institutes of Health (AI083365 to TGB, AI122363 to JLB) and funds from Howard Hughes Medical Institute.

Data Availability Statement

The data that support the findings of this study are available from the corresponding author upon reasonable request.

REFERENCES

Baba T, Ara T, Hasegawa M, Takai Y, Okumura Y, Baba M, et al. (2006) Construction of *Escherichia coli* K-12 in-frame, single-gene knockout mutants: the Keio collection. Mol Syst Biol 2: 2006.0008.

Bendezú FO, and de Boer PAJ (2008) Conditional lethality, division defects, membrane involution, and endocytosis in *mre* and *mrd* shape mutants of *Escherichia coli*. J Bacteriol 190: 1792–1811. [PubMed: 17993535]

Bernhardt TG, and de Boer PAJ (2004) Screening for synthetic lethal mutants in *Escherichia coli* and identification of EnvC (YibP) as a periplasmic septal ring factor with murein hydrolase activity. Molecular Microbiology 52: 1255–1269. [PubMed: 15165230]

Bertsche U, Breukink E, Kast T, and Vollmer W (2005) In vitro murein peptidoglycan synthesis by dimers of the bifunctional transglycosylase-transpeptidase PBP1B from *Escherichia coli*. J Biol Chem 280: 38096–38101. [PubMed: 16154998]

Cho H, Wivagg CN, Kapoor M, Barry Z, Rohs PDA, Suh H, et al. (2016) Bacterial cell wall biogenesis is mediated by SEDS and PBP polymerase families functioning semi-autonomously. Nat Microbiol 1: 16172. [PubMed: 27643381]

Fenton AK, Mortaji El, L., Lau DTC, Rudner DZ, and Bernhardt TG. (2016) CozE is a member of the MreCD complex that directs cell elongation in *Streptococcus pneumoniae*. Nat Microbiol 2: 16237. [PubMed: 27941863]

Heidrich C, Ursinus A, Berger J, Schwarz H, and Höltje J-V (2002) Effects of multiple deletions of murein hydrolases on viability, septum cleavage, and sensitivity to large toxic molecules in *Escherichia coli*. J Bacteriol 184: 6093–6099. [PubMed: 12399477]

Höltje J-V (1998) Growth of the Stress-Bearing and Shape-Maintaining Murein Sacculus of Escherichia coli. Microbiol Mol Biol Rev 62: 181–203. [PubMed: 9529891]

Ishino F, Mitsui K, Tamaki S, and Matsuhashi M (1980) Dual enzyme activities of cell wall peptidoglycan synthesis, peptidoglycan transglycosylase and penicillin-sensitive transpeptidase, in purified preparations of *Escherichia coli* penicillin-binding protein 1A. Biochem Biophys Res Commun 97: 287–293. [PubMed: 7006606]

Jorgenson MA, Chen Y, Yahashiri A, Popham DL, and Weiss DS (2014) The bacterial septal ring protein RlpA is a lytic transglycosylase that contributes to rod shape and daughter cell separation in *Pseudomonas aeruginosa*. Molecular Microbiology 93: 113–128. [PubMed: 24806796]

Karimova G, Pidoux J, Ullmann A, and Ladant D (1998) A bacterial two-hybrid system based on a reconstituted signal transduction pathway. Proc Natl Acad Sci USA 95: 5752–5756. [PubMed: 9576956]

Kato J, Suzuki H, and Hirota Y (1985) Dispensability of either penicillin-binding protein-1a or -1b involved in the essential process for cell elongation in *Escherichia coli*. Mol Gen Genet 200: 272–277. [PubMed: 2993822]

Kraft AR, Prabhu J, Ursinus A, and Höltje JV (1999) Interference with murein turnover has no effect on growth but reduces beta-lactamase induction in *Escherichia coli*. J Bacteriol 181: 7192–7198. [PubMed: 10572120]

Kraft AR, Templin MF, and Höltje JV (1998) Membrane-bound lytic endotransglycosylase in *Escherichia coli*. J Bacteriol 180: 3441–3447. [PubMed: 9642199]

Land AD, and Winkler ME (2011) The requirement for pneumococcal MreC and MreD is relieved by inactivation of the gene encoding PBP1a. J Bacteriol 193: 4166–4179. [PubMed: 21685290]

Lloubès R, Cascales E, Walburger A, Bouveret E, Lazdunski C, Bernadac A, and Journet L (2001) The Tol-Pal proteins of the *Escherichia coli* cell envelope: an energized system required for outer membrane integrity? Res Microbiol 152: 523–529. [PubMed: 11501670]

Markovski M, Bohrhunter JL, Lupoli TJ, Uehara T, Walker S, Kahne DE, and Bernhardt TG (2016) Cofactor bypass variants reveal a conformational control mechanism governing cell wall polymerase activity. Proc Natl Acad Sci USA 113: 201524538–4793.

Meeske AJ, Riley EP, Robins WP, Uehara T, Mekalanos JJ, Kahne D, et al. (2016) SEDS proteins are a widespread family of bacterial cell wall polymerases. Nature 537: 634–638. [PubMed: 27525505]

Nakagawa J, Tamaki S, Tomioka S, and Matsuhashi M (1984) Functional biosynthesis of cell wall peptidoglycan by polymorphic bifunctional polypeptides. Penicillin-binding protein 1Bs of *Escherichia coli* with activities of transglycosylase and transpeptidase. J Biol Chem 259: 13937–13946. [PubMed: 6389538]

Paradis-Bleau C, Markovski M, Uehara T, Lupoli TJ, Walker S, Kahne DE, and Bernhardt TG (2010) Lipoprotein cofactors located in the outer membrane activate bacterial cell wall polymerases. Cell 143: 1110–1120. [PubMed: 21183074]

Rohs PDA, Buss J, Sim SI, Squyres GR, Srisuknimit V, Smith M, et al. (2018) A central role for PBP2 in the activation of peptidoglycan polymerization by the bacterial cell elongation machinery. PLoS Genet 14: e1007726. [PubMed: 30335755]

Sauvage E, Kerff F, Terrak M, Ayala JA, and Charlier P (2008) The penicillin-binding proteins: structure and role in peptidoglycan biosynthesis. FEMS Microbiol Rev 32: 234–258. [PubMed: 18266856]

Scheurwater E, Reid CW, and Clarke AJ (2008) Lytic transglycosylases: bacterial space-making autolysins. Int J Biochem Cell Biol 40: 586–591. [PubMed: 17468031]

Taguchi A, Welsh MA, Marmont LS, Lee W, Sjodt M, Kruse AC, et al. (2019) FtsW is a peptidoglycan polymerase that is functional only in complex with its cognate penicillin-binding protein. Nat Microbiol 2: a000414–594.

Tokuda H, and Matsuyama S-I (2004) Sorting of lipoproteins to the outer membrane in *E. coli*. Biochim Biophys Acta 1693: 5–13. [PubMed: 15276320]

Tsui HCT, Zheng JJ, Magallon AN, Ryan JD, Yunck R, Rued BE, et al. (2016) Suppression of a Deletion Mutation in the Gene Encoding Essential PBP2b Reveals a New Lytic Transglycosylase Involved in Peripheral Peptidoglycan Synthesis in Streptococcus pneumoniae D39. Molecular Microbiology 100:1039–1065 [PubMed: 26933838]

Typas A, Banzhaf M, Gross CA, and Vollmer W (2012) From the regulation of peptidoglycan synthesis to bacterial growth and morphology. Nat Rev Microbiol 10: 123–136.

Typas A, Banzhaf M, van den Berg van Saparoea B, Verheul J, Biboy J, Nichols RJ, et al. (2010) Regulation of peptidoglycan synthesis by outer-membrane proteins. Cell 143: 1097–1109. [PubMed: 21183073]

van Heijenoort J (2011) Peptidoglycan hydrolases of *Escherichia coli*. Microbiol Mol Biol Rev 75:636–663. [PubMed: 22126997]

Ye XY, Lo MC, Brunner L, Walker D, Kahne D, and Walker S (2001) Better substrates for bacterial transglycosylases. J Am Chem Soc 123: 3155–3156. [PubMed: 11457035]

Yousif SY, Broome-Smith JK, and Spratt BG (1985) Lysis of Escherichia coli by beta-lactam antibiotics: deletion analysis of the role of penicillin-binding proteins 1A and 1B. J Gen Microbiol 131: 2839–2845. [PubMed: 3906031]

Yunck R, Cho H, and Bernhardt TG (2015) Identification of MltG as a potential terminase for peptidoglycan polymerization in bacteria. Molecular Microbiology 99: 700–718. [PubMed: 26507882]

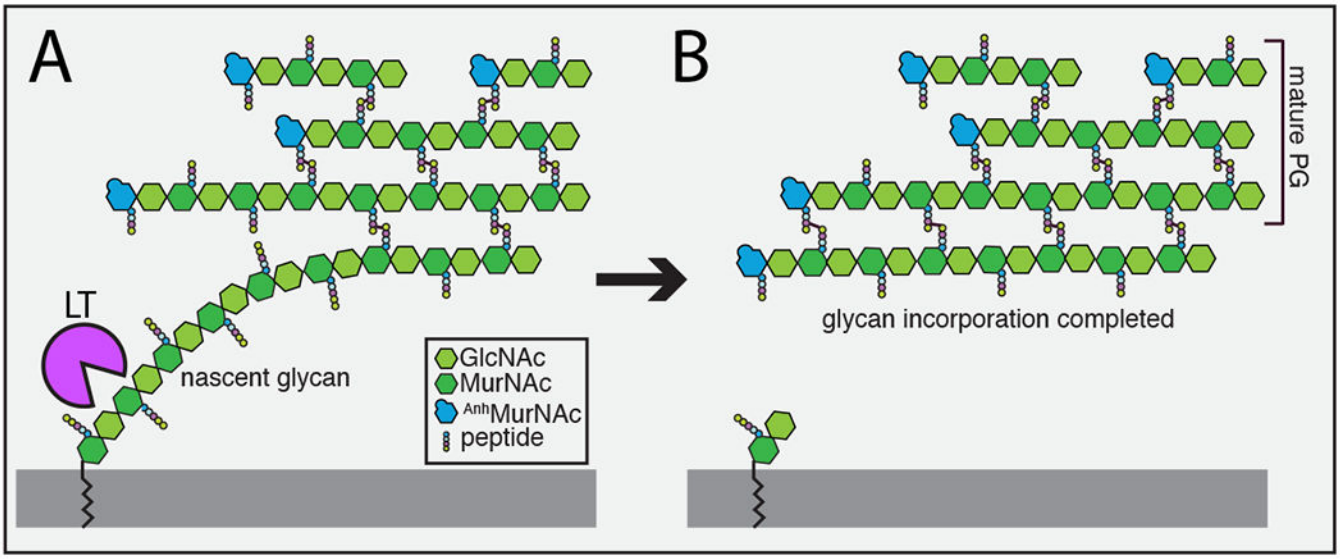

Figure 1. Lytic transglycosylase activity and the completion of PG glycan incorporation.

Shown is a diagram illustrating the final step required for the completion of PG glycan strand incorporation into the mature PG matrix. PG glycans are synthesized from the lipid-linked precursor lipid II such that the product of polymerization is a lipid-anchored glycan chain. Enzymes called lytic transglycosylases (LTs) are thought to release this membrane tethered polymer by cleaving within the strand and creating an anhydro-MurNAc end. It is unclear whether LT cleavage occurs following the completion of glycan polymerization or as the strand is being synthesized.

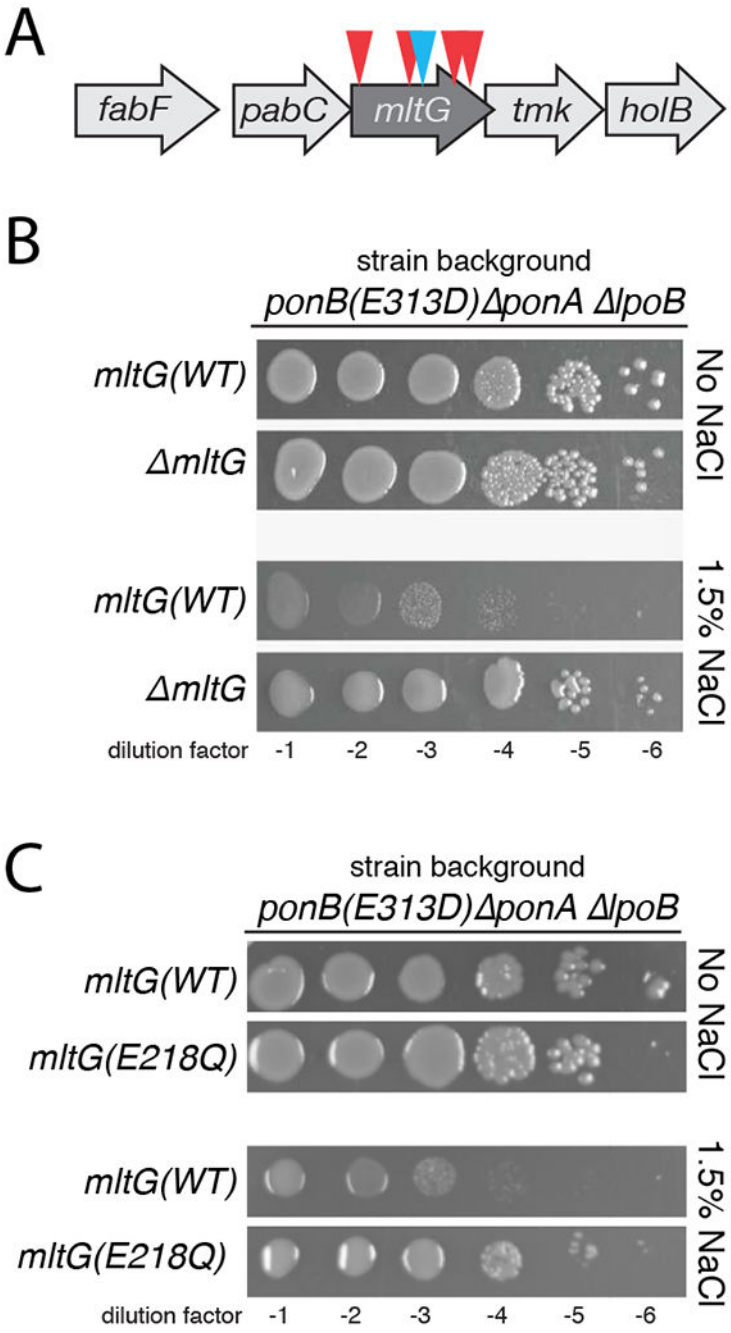

Figure 2. Loss of MltG function suppresses a lethal aPBP activity deficit

(A) Shown is a diagram of the *mltG* locus with the approximate location of transposon insertions resulting in the suppression of the salt sensitivity of strain MM119 [Δ*lpoB* Δ*lponA ponB(E313D)*] depicted as arrowheads. Insertions with transcription of the resistance cassette in the same orientation as *mltG* are in blue, and those with transcription in the reverse orientation are in red. (B) Cells of MM119 and its Δ*mltG* derivative were grown overnight in LB0N. Cells in the resulting cultures were diluted to an OD_{600} of 1.0 in LB0N, and serially diluted. An aliquot (5 μL) of each dilution was spotted onto LB agar

plates containing the indicated percentage of NaCl. Plates were incubated at 30°C for 20 hours prior to imaging. (C) Cells of MM119 and its *mltG(E218Q)* derivative were plated and imaged as in panel (B).

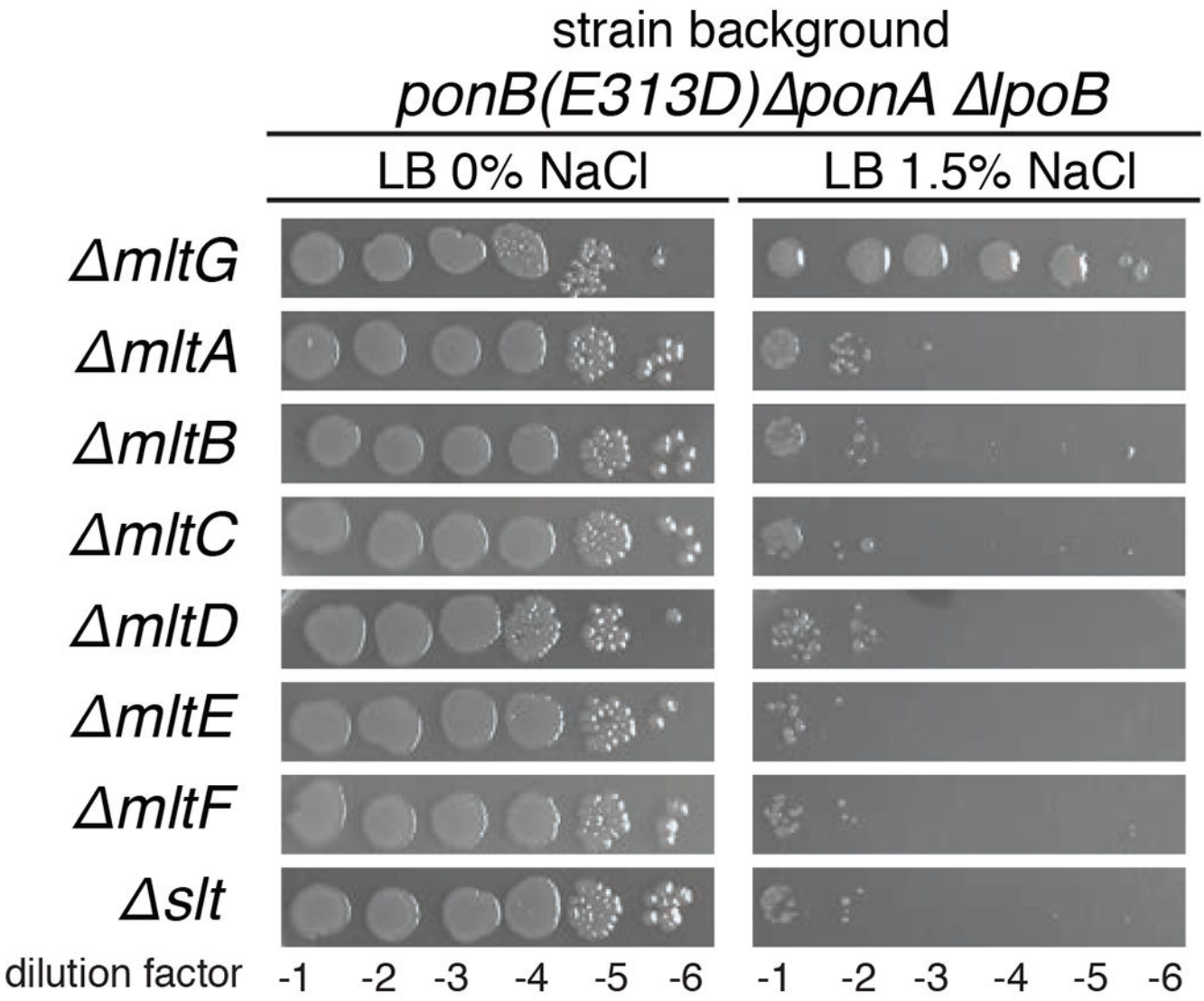

Figure 3. Inactivation of other LTs fails to suppress the aPBP defect of MM119.

Cells of Cells of MM119 [Δ*lpoB* Δ*ponA ponB(E313D)*] and its Δ*mltA*, Δ*mltB*, Δ*mltC*, Δ*mltD*, Δ*mltE*, Δ*mltF*, Δ*mltG*, and Δ*slt70* derivatives were grown, diluted, and plated on LB agar as in Figure 2.

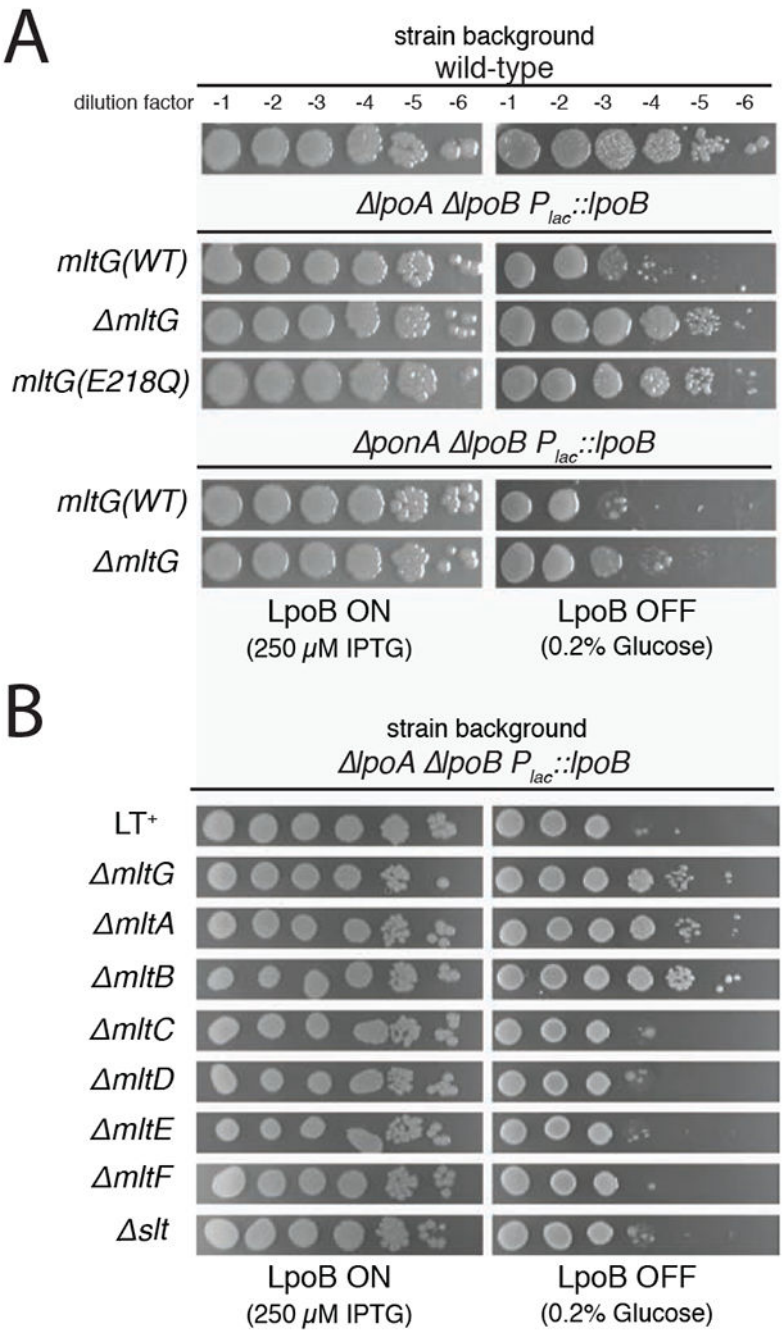

Figure 4. Loss of MltG function suppresses the lethal inactivation of aPBP activators.

(A) Cells of TB28 [WT], CB68 [Δ*lpoB* Δ*lpoA* (P_{lac}::*lpoB-sfgfp*)], JLB23 [Δ*lpoB* Δ*lpoA* Δ*mltG* (P_{lac}::*lpoB-sfgfp*)], and JLB24 [Δ*lpoB* Δ*ponA* Δ*mltG* (P_{lac}::*lpoB-sfgfp*)], CB71 [Δ*lpoB* Δ*ponA* (P_{lac}::*lpoB-sfgfp*)], and JLB24 [Δ*lpoB* Δ*ponA* Δ*mltG* (P_{lac}::*lpoB-sfgfp*)] were grown overnight in LB broth supplemented with 250 μM IPTG. Overnight cultures were diluted and plated on the indicated LB agar medium as in Figure 2. Plates were incubated at 37°C for 20 hours prior to imaging. (B) Cells of JLB44 [Δ*lpoB* Δ*lpoA*

(P_{lac}::*lpoB-sfgfp*)] and its Δ*mltG*, Δ*mltA*, Δ*mltB*, Δ*mltC*, Δ*mltD*, Δ*mltE*, Δ*mltF*, and Δ*slt70* derivatives were grown, diluted, and plated as in panel A.

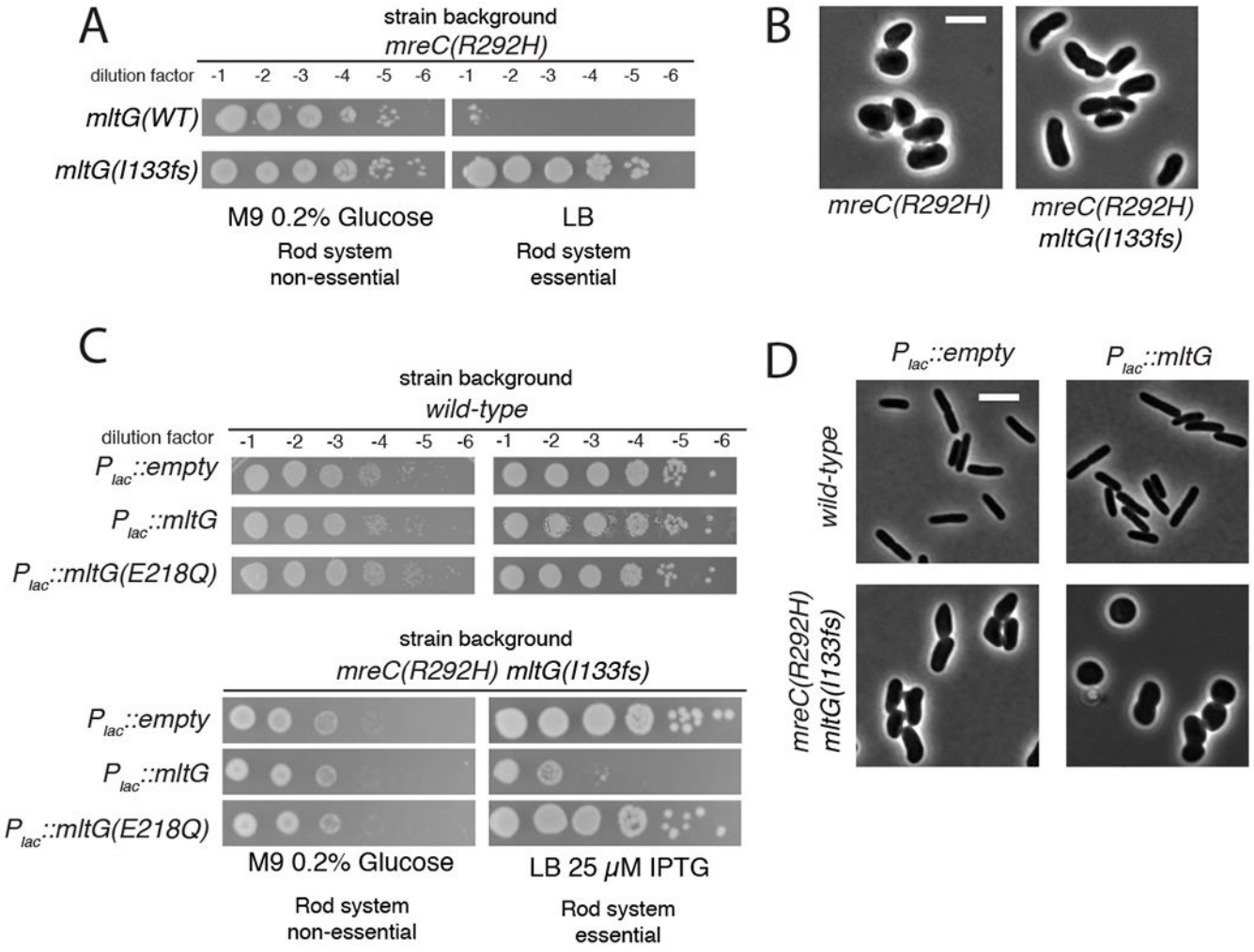

Figure 5. Loss of MltG function suppresses an elongation system defect.

(A) Cells of PR5 [*mreC*(R292H)] and its *mltG(I133fs*) derivative were grown overnight in M9 medium supplemented with 0.2% casamino acids and 0.2% glucose at 30°C. Cells in the resulting cultures were harvested, washed once in an equal volume of M9 supplemented with 0.2% casamino acids, and resuspended in M9 supplemented with 0.2% casamino acids at an 0D600 of 1.0. The resulting cell suspensions were subjected to serial dilution, and 5 μL of each dilution were spotted onto M9 agar plates supplemented with 0.2% casamino acids or LB agar plates, as indicated. Plates were incubated at 30°C for 48 house prior to imaging. (B) The same cells were grown in M9 medium supplemented with with 0.2% casamino acids and 0.2% maltose overnight at 30°C, diluted to an OD_{600} of 0.05 in the same medium, and grown to an OD_{600} of 0.2. Cells were then harvested by centrifugation and resuspended in LB to a final OD_{600} of 0.025. These cultures were grown at 30°C to an OD_{600} of approximately 0.2. Cells were then fixed, and imaged on M9 agar pads as described previously (Rohs et al., 2018). (C) Cells of TB28 [WT] or PR36 [*mreC(R292H) mltG(I133fs)*] containing the indicated expression plasmids pRY47 [P_{lac}::empty], pRY42 [P_{lac}::*mltG*], or pRY73 [P_{lac}::*mltG(E218Q)*] were grown overnight in M9 medium supplemented with 0.2% casamino acids and 0.2% arabinose and 25

μg/mL chloramphenicol at 30°C (PR36 background) or LB supplemented with 25 μg/mL chloramphenicol and 0.2% glucose at 37°C (TB28 background). Cells were then washed, diluted, and plated as in panel A, except the medium contained 25 μg/mL chloramphenicol to select for the plasmids. Note that the M9 0.2% glucose plates were only incubated overnight before imaging. Therefore, although cell growth appears to be reduced relative to panel A, plating efficiency is actually unchanged. (D) The same cells as in panel C were grown and imaged as in panel B, except that the medium was supplemented with 25 μM IPTG and 25 μg/mL chloramphenicol.

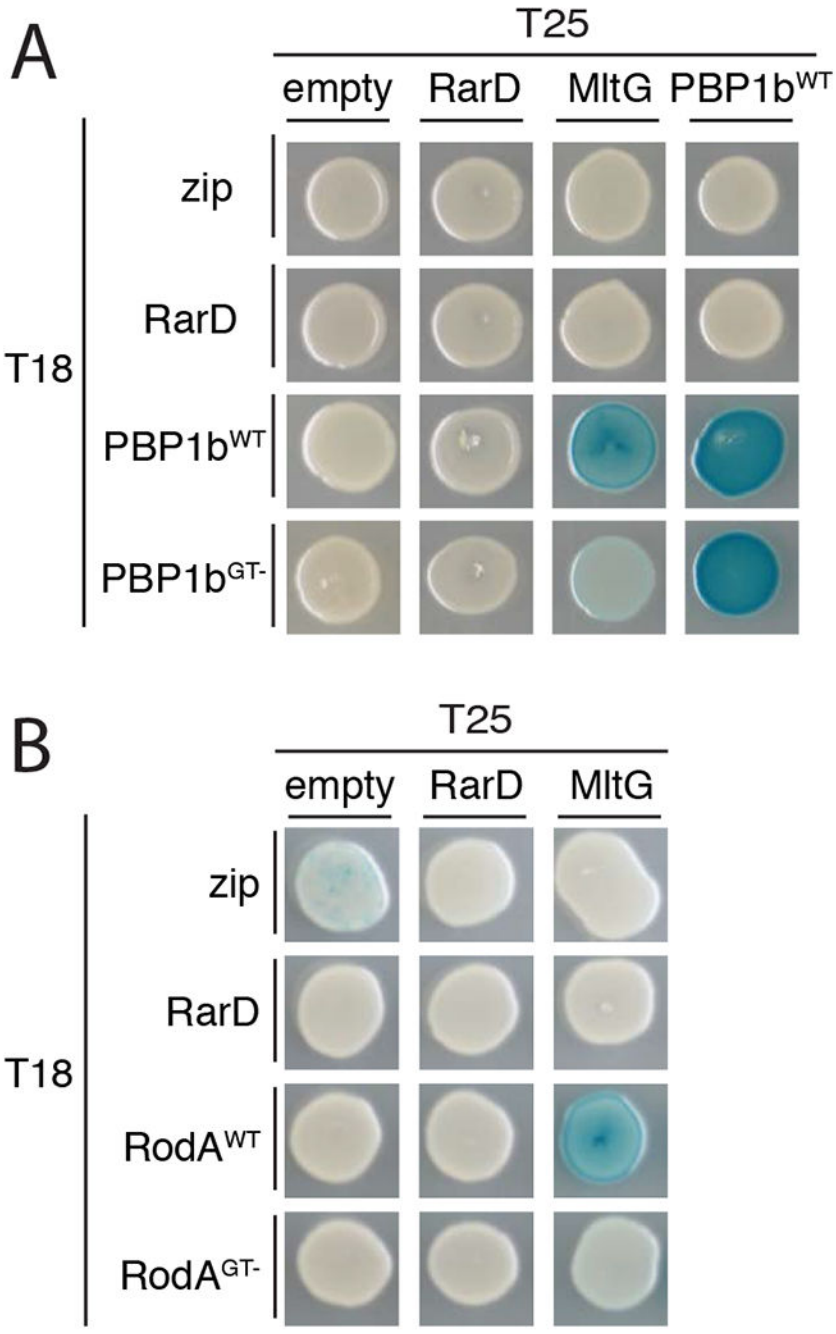

Figure 6. BACTH analysis of MltG interaction with PG polymerases.

BTH101 cells containing plasmids producing the indicated T25 and T18 fusions were grown in LB with 50 μg/mL ampicillin, 25 μg/mL kanamycin and 1 mM IPTG. An aliquot (5 μL) of each overnight culture was spotted on LB agar with 50 μg/mL ampicillin, 25 μg/mL kanamycin, 1 mM IPTG, and 80 μg/mL X-gal. Plates were incubated at room temperature for 2 days then moved to 4°C overnight to assist color development, before being imaged.

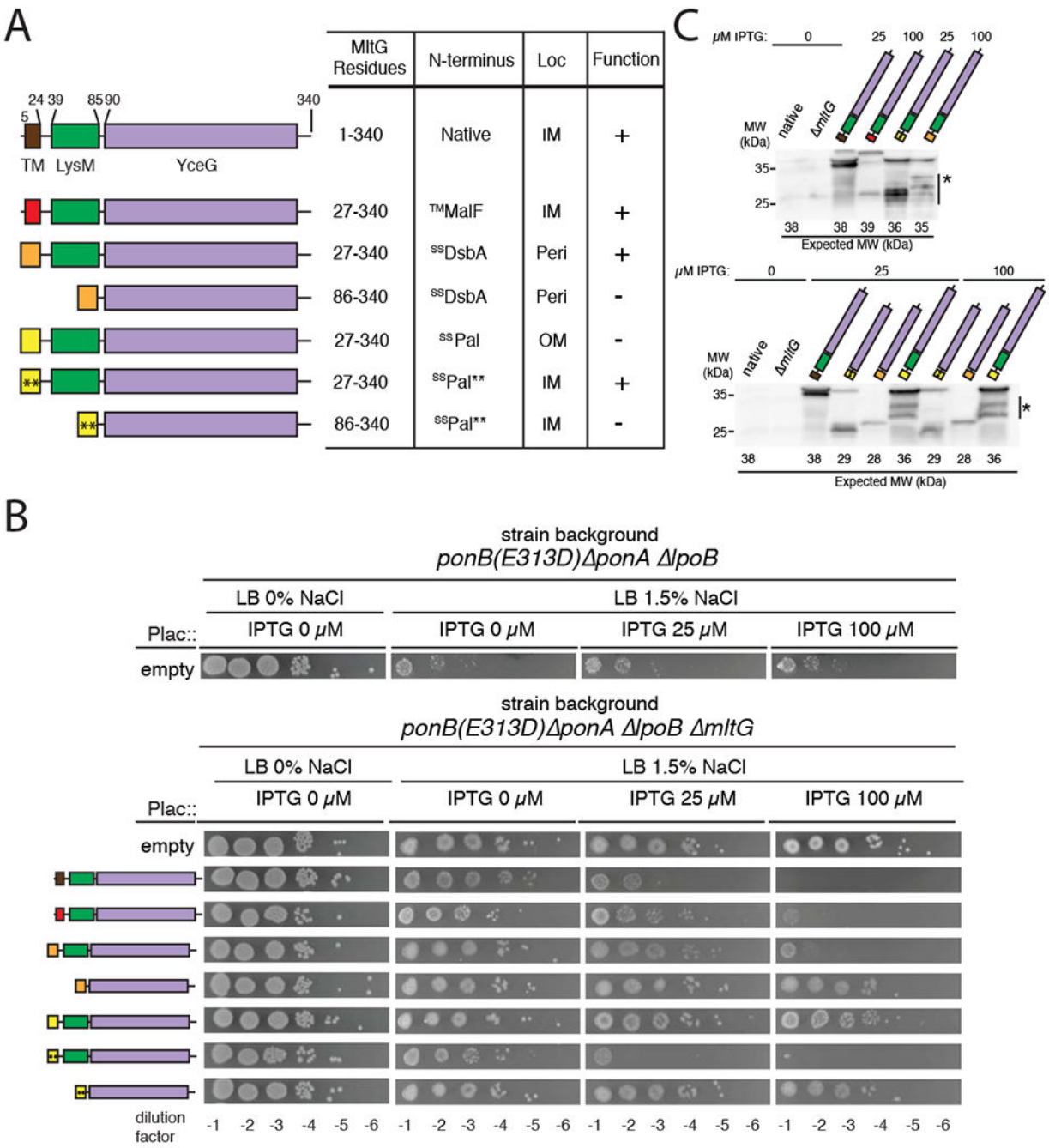

Figure 7. MltG requires access to the inner membrane.

(A) Diagram of MltG expression constructs used for functional analysis. The double asterisks (**) indicate that the Pal signal sequence has been altered (S23D, S24E) to promote inner membrane retention. (B) Cells of MM119 [Δ*lpoB* Δ*ponA ponB(E313D)*] or its Δ*mltG* derivative with the indicated plasmids were were grown overnight in LB0N supplemented with 25 μg/mL chloramphenicol and 0.2% glucose. Cells in the resulting cultures were diluted and spotted on the indicated medium as described in Figure 2. Plates were incubated at 37°C

for 20 hours prior to imaging. Plasmids used were: pRY47 [P_{lac}::empty], pRY42 [P_{lac}::*mltG*], pRY116 [P_{lac}::*dsbA(1-71)-mltG(27-340)*], pRY117 [P_{lac}::*pal(1-84, S23D, S24E)-mltG(27-340)*], pRY118 [P_{lac}::*dsbA(1-71)-mltG(86-340)*], pRY119 [P_{lac}::*pal(1-84, S23D, S24E)-mltG(86-340)*], pRY125 [P_{lac}::*malF(1-113)-mltG(27-340)*], or pJLB81 [P_{lac}::*pal(1-84)-mltG(27-340)*]. (C) Strains used in (B) were grown overnight in LB0N supplemented with 25 μg/mL chloramphenicol and the indicated concentration of IPTG. The accumulation of MltG proteins was then determined by immunoblotting with anti-MltG antisera. Asterisks indicate the position of what are likely to be cleavage products of several of the MltG variants.